ChemComm

COMMUNICATION

View Article Online
View Journal | View Issue

Cite this: *Chem. Commun.*, 2021, 57, 5538

Received 17th March 2021,
Accepted 27th April 2021

DOI: 10.1039/d1cc01431e

rsc.li/chemcomm

Eshelby untwisting†

Xiaodi Zhong,‡ Hengyu Zhou,‡ Chao Li, Alexander G. Shtukenberg, Michael D. Ward* and Bart Kahr*

The concept of Eshelby untwisting, the effect of an axial screw dislocation driving an intrinsically twisted nanocrystal towards a straighter configuration more consistent with long–range translational symmetry, is introduced here. Force-field simulations of nanorods built from the enantiomorphous (space groups, $P3_121$ and $P3_221$) crystal structures of benzil (C_6H_5–C(O)–C(O)–C_6H_5) were previously shown to twist in opposite directions, even in the absence of dislocations. Here, both right- and left-handed screw dislocations were introduced into benzil nanorods *in silico*. For rods built from the $P3_221$ enantiomorph, dislocations with negative Burgers vectors increased the right-handed twisting already present in the intrinsically twisted structures without dislocations, whereas dislocations with positive Burgers vectors drove the twisted structure back towards a straight configuration, untwisting. In the dynamic simulations, the $P3_221$ helicoid endowed with a positive Burgers vector ultimately twisted back through the straight configuration, until a helicoid of opposite sense from that of the starting structure, was obtained. The bearing of these observations on the propensity of small crystals to adopt non-polyhedral morphologies is discussed.

The relief of stress associated with an axial screw dislocation in a slender crystal can create a torque that results in an overall twist named for Eshelby, who first analysed mechanical distortions of this kind.[1,2] Eshelby twisting is a well-studied phenomenon in materials science[3–5] that also has been modelled computationally.[6–8] Previously, we studied the Eshelby mechanism in models of enantiomorphous, molecular nanocrystals of iodoform (CHI_3), *in silico*.[9,10] We were motivated to characterize differences in twisting, if any, for dislocations with oppositely signed Burgers vectors (+**b** and −**b**) introduced into the *same* enantiomorph.[9,10] Symmetry requires that such twists, while opposite, must not be precisely equal in absolute amplitude. We did not observe meaningful differences in molecular dynamics (MD) simulations.

More recently, we simulated the geometry of molecular nanocrystals that were twisted, in the *absence* of dislocations.[11,12] Benzil (Fig. 1), which crystallizes in the enantiomorphous space groups $P3_121$ and $P3_221$, is one of many molecular crystals that can grow with helicoidal morphologies in fibrous radial bundles known as banded spherulites.[13] There is no evidence that these crystals are twisted by the Eshelby mechanism, however, especially since innumerable crystals twist in sync, forming concentric bands. Dislocation formation is stochastic.[14,15]

While there are mechanistic questions associated with the growth of crystalline helicoids,[16,17] when crystals are very small they do not need to have long–range translational symmetry. Simulations reveal that benzil nanocrystals are not represented by a traditional crystallographic lattice,[11] consistent with the helicoidal twisting in its slender molecular crystals.[11–13] Computations at the nanoscale therefore can be used to compare the contributions of various mechanisms to twisting as well as untwisting, processes well documented in our laboratory.[18,19] If a computational model of a small crystal is

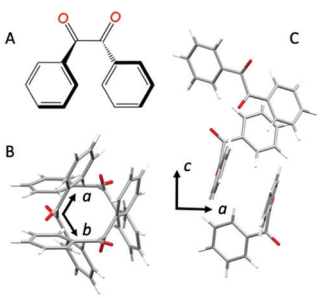

Fig. 1 (A) Benzil molecule, and crystal structure in space group $P3_121$, $Z = 3$ viewed along (B) and normal to (C) the unique axis.

Department of Chemistry and the Molecular Design Institute, New York University, 100 Washington Square East, New York, NY 10003-6688, USA.
E-mail: mdw3@nyu.edu, bart.kahr@nyu.edu

† Electronic supplementary information (ESI) available. See DOI: 10.1039/d1cc01431e

‡ Xiaodi Zhong and Hengyu Zhou contributed equally to this work.

twisted intrinsically under the constraints of a force field, building screw dislocations of opposite signs into the model should lead to Eshelby twisting and Eshelby untwisting, the latter term specifying a return of the intrinsically twisted crystal to a configuration more consistent with long–range translational symmetry. In other words, a +**b** screw dislocation should further twist an intrinsically twisted nanorod of a given enantiomorph, while a −**b** screw dislocation should *untwist* that rod, and *vice versa*. This proposition is evaluated herein.

Hexagonal rods of benzil (space groups $P3_121$ and $P3_221$) were built *in silico* with lattice parameters determined at 100 K: $a = b = 8.356(3)$ Å and $c = 13.375(6)$ Å.[20] The rods were 15 unit cells along the c axis, and 4, 6, 8, or 10 unit cells along a. Screw dislocations were set at Burgers vector $\mathbf{b} = [000 \pm 1]$ and generated by displacing molecules along a shear plane from zero to **b**, with the dislocation cores extended evenly over 3 unit cells for all rods, regardless of rod size.[21] For a right-handed screw dislocation, molecules outside the dislocation core were raised uniformly along [0001] from zero to **b** when rotating by 2π around the core, producing shears in the $(2\bar{1}\bar{1}0)$ or $(10\bar{1}0)$ planes. The magnitude of the displacement, z, of the molecules along c was calculated as: $z = b/(2\pi)$, increasing by $b/3$ for each of three turns. For a left-handed screw dislocation with Burgers vector $\mathbf{b} = c\ [000\bar{1}]$, z was calculated the same way, but the molecules were lowered.

Generalized amber force field (GAFF)[22,23] geometry optimizations and MD simulations were conducted with the large-scale atomic/molecular massively parallel simulator (LAMMPS).[24] The benzil nanorods were located in the centre of a simulation box and the distances between the crystal surfaces and the box boundaries were >15 Å in orthogonal directions. Partial atomic charges were derived from a restrained electrostatic potential (RESP) calculation with the HF/6-31G* basis set using the R.E.D. web server.[25–28] The General Utility Lattice Program (GULP) was used to calculate the four–body interaction parameters.[29,30] Mechanical distortions were primarily non-activated, barrier-free processes. Conjugate gradient energy minimisation was achieved with a relative energy tolerance of 10^{-8}. MD was

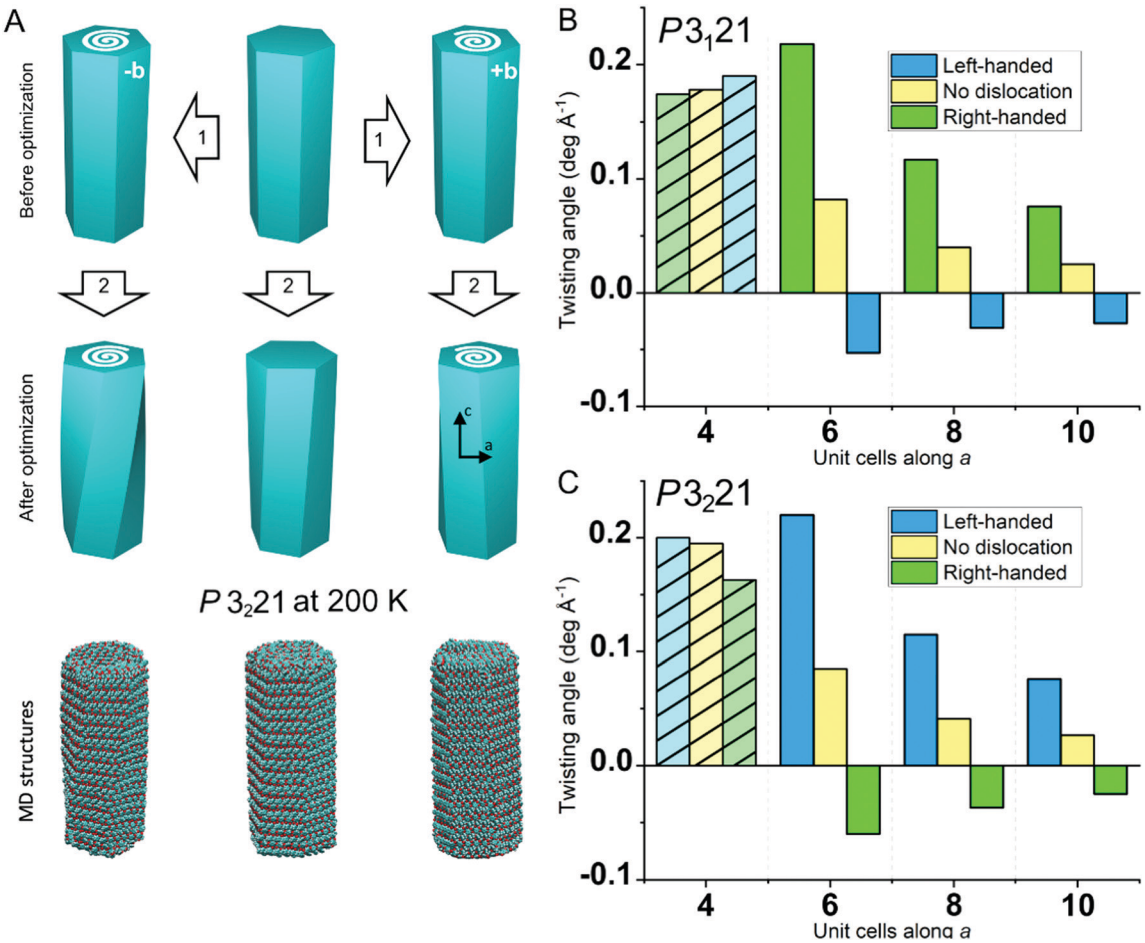

Fig. 2 Schematic drawings of Eshelby twisting and untwisting and corresponding atomistic models of benzil nanorods in the space group $P3_221$ (A) and twisting angles of the rods in actual simulations (B and C). In (A), step 1 is the introduction of the screw dislocations computationally. Step 2 is relaxation of the straight structures (centres of middle rows) to produce intrinsically twisted structures, of Eshelby twisting and Eshelby untwisting, left and right of middle rows, respectively. The bottom row depicts the simulation results for a $P3_221$ rod of size 6 × 6 × 15 unit cells at 200 K. In (B and C), twist angles for 4 × 4 × 15 unit cells are depicted in faded colors to denote that the dislocations moved out of the rods, precluding the use of the Eshelby twisting concept.

performed at 200 K with the NVE microcanonical ensemble controlled by a Langevin thermostat with 1 fs steps.

Calculation of twisting angles were based on molecules inside the crystal. Cells in layers positioned at 1/4 and 3/4 along c of the crystal were selected, as in Fig. S1 (ESI†) and discussion therein. These angles were averaged over the last nanosecond of the simulation. Rods sometimes become trapped in local minima during non-activated Eshelby untwisting at low temperature or during MD simulations below 100 K (Fig. S2, ESI†). Above 200 K, smaller rods showed signs of melting. Simulations at 200 K was the best compromise (Fig. S3, ESI†) between reaching minima required by symmetry and structural integrity. The cut-off distance for pairwise Lennard Jones interactions was set to 12.5 Å, while the electrostatic interactions beyond 12.5 Å were calculated in reciprocal space using the particle–particle particle-mesh k-space method. This process was efficient and accurate when the results were compared to simulations of undislocated benzil[11] without cut-offs. Trajectories were recorded every 500 fs for periods of 5 ns until the twisting angle was unchanging within $<2\%$ over a period of 0.2 ns. The simulation results were indifferent to the choice of $(01\bar{1}0)$ and $(1\bar{2}10)$ shear planes, both parallel to $<0001>$ (see Fig. S4, ESI†). Previous simulations of iodoform were indifferent to the choice of slip plane as well.[9]

Twisted microfibers of benzil can be crystallized from the melt.[11] Moreover, force field calculations suggested that benzil nanocrystals without dislocations were intrinsically twisted.[11] Herein, we describe simulations in which trigonal crystals were dislocated with $[000 \pm 1]$ Burgers vectors and subsequently allowed to relax. This workflow is illustrated schematically in Fig. 2A, accompanied by the actual simulation results for a $P3_221$ benzil rod of six-unit cells in the a and b directions at 200 K. The pitch, defined as the length needed for a 2π rotation (μm), increased linearly with increasing cross-sectional area, consistent with previous findings.[11,12]

According to Eshelby's theory,[1,2] an axial screw dislocation in a slender crystal creates an elastic stress field that may be partially relaxed by continuous twisting. The degree of twisting per unit length induced by the torque formed in a cylindrical rod is $\alpha = kb/A$, where α is the Eshelby twisting angle, b is the length of Burgers vector, A is the cross-sectional area of the cylinder, and $k = 1.015$ is a geometrical constant for a regular hexagonal cross section. Twist angles of nanorods were calculated by MD simulations at 200 K. A $6 \times 6 \times 15$ unit cell benzil nanocrystal that intrinsically twisted by $\theta = 0.085$ deg Å^{-1} will be further distorted by screw dislocations, enhancing $(\theta + \alpha)$ or diminishing $(\theta - \alpha)$ the twist according to the sign of $\boldsymbol{b}$ and the enantiomorph modelled. A right-handed dislocation $(+\boldsymbol{b})$ introduced to a $P3_221$ rod decreased the twist to -0.060 deg Å^{-1} (Fig. 2); the crystal became straighter while the twisting direction was reversed. A Burgers vector $-\boldsymbol{b}$ increased the intrinsic twist to 0.22 deg Å^{-1}. The degree of twisting, α, is approximately 0.135 deg Å^{-1} for further twisting and -0.145 deg Å^{-1} for untwisting. Despite the geometrical frustration that twists the rod without any dislocations, heterochiral twists were opposite in sign and nearly so in magnitude, consistent with Eshelby's analysis.[1,2]

Dislocations were expelled from rods with only 4-unit cells along a. For this reason, the twist is indifferent to the sense of the dislocation incorporated into these models. These rods, denoted with cross hatching in the bar graphs in Fig. 2B and C, achieve twisting angles comparable to the intrinsic twist.

The potential energies (PEs) of individual molecules are denoted by colour in Fig. S5 (ESI†). The molecules on the surfaces are incompletely coordinated with higher PEs as expected. The PEs of molecules within the dislocation cores were larger by *ca.* 0.1–0.2 eV molecule^{-1}. This excess energy is quickly dissipated, and it dissipated more quickly for right-handed dislocations in $P3_221$, as depicted. The total potential energy (energy per molecule) for $6 \times 6 \times 15$ rods with $a - \boldsymbol{b}$ dislocation (further twisted) was 18.98 eV (0.005 eV) compared with the undislocated model. With $a + \boldsymbol{b}$ dislocation (untwisted), the relative energy was 43.51 eV (0.011 eV), also compared to the undislocated model. The aggregate energies indicate that further twisting by the Eshelby mechanism is less of a thermodynamic burden than the untwisting. Equal and opposite behaviour is observed in $P3_121$ with dislocations of opposite signs. At 200 K, conformations were comparable near and far from the core (Fig. S6, ESI†), yet overall, the mechanical distortions were persistent.[10] The observations suggest that breaking the symmetry of the surfaces $\{10\bar{1}0\}$, observed in non-activated minimisations, is unlikely to be a cause of the twisting.[31]

In sum, simulations showed that intrinsically twisted nanocrystals of benzil undergo Eshelby twisting and untwisting by screw dislocations of opposite signs. The influences of $\pm\boldsymbol{b}$ dislocations are opposite but not equal in absolute magnitude, as the starting structures are not only molecularly chiral, but mechanically chiral (structures are twisted) to begin with. Rods further twisted by screw dislocations have smaller potential energies than those forced to untwist.

This work was primarily supported by the New York University Materials Research Science and Engineering Center (MRSEC) program of the US National Science Foundation under award DMR-1420073. Funding was also provided by DMR-2003968. Thanks are extended to our friends at Curtin University, Perth, Professors Andrew Rohl, Paolo Raiteri, and Julian Gale for sage advice on methodologies. The idea for the study was conceived by B. K., A. G. S., and M. D. W. X. Z., H. Z., and C. L. performed the M. D. simulation. All authors contributed to the analysis of the data. The manuscript was written by H. Z., X. Z., M. D. W., A. G. S., and B. K.

Conflicts of interest

There are no conflicts to declare.

Notes and references

1 J. D. Eshelby, *J. Appl. Phys.*, 1953, **24**, 176–179.
2 J. D. Eshelby, *Philos. Mag.*, 1958, **3**, 440–447.
3 M. J. Bierman, Y. K. A. Lau, A. V. Kvit, A. L. Schmitt and S. Jin, *Science*, 2008, **320**, 1060–1063.

4 S. A. Morin, M. J. Bierman, J. Tong and S. Jin, *Science*, 2010, **328**, 476–480.
5 J. Zhu, H. Peng, A. F. Marshall, D. M. Barnett, W. D. Nix and Y. Cui, *Nat. Nanotechnol.*, 2008, **3**, 477–481.
6 I. Nikiforov, D. B. Zhang and T. Dumitrică, *J. Phys. Chem. Lett.*, 2011, **2**, 2544–2548.
7 E. Akatyeva and T. Dumitrică, *Phys. Rev. Lett.*, 2012, **109**, 035501.
8 D. B. Zhang, E. Akatyeva and T. Dumitrică, *Phys. Rev. B: Condens. Matter Mater. Phys.*, 2011, **84**, 115431.
9 I. Olson, A. Shtukenberg, B. Kahr and M. D. Ward, *Rev. Prog. Phys*, 2018, **81**, 096501.
10 C. Li, A. G. Shtukenberg, D. J. Carter, X. Cui, I. Olson, A. L. Rohl, J. D. Gale, P. Raiteri and B. Kahr, *J. Phys. Chem. C*, 2018, **122**, 25085–25091.
11 C. Li, A. G. Shtukenberg, E. Efrati, L. Vogt-Maranto, P. Raiteri, J. D. Gale, A. L. Rohl and B. Kahr, *J. Phys. Chem. C*, 2020, **124**, 15616–15624.
12 A. Haddad, H. Aharoni, E. Sharon, A. G. Shtukenberg, B. Kahr and E. Efrati, *Soft Matter*, 2019, **15**, 116–126.
13 A. G. Shtukenberg, Y. Yang, X. Zhu and B. Kahr, *Cryst. Growth Des.*, 2020, **20**, 6186–6197.
14 X. Zhong, A. G. Shtukenberg, T. Hueckel, B. Kahr and M. D. Ward, *Cryst. Growth Des.*, 2018, **18**, 318–323.
15 X. Zhong, A. G. Shtukenberg, M. Liu, I. A. Olson, M. Weck, M. D. Ward and B. Kahr, *Cryst. Growth Des.*, 2019, **19**, 6649–6655.
16 A. G. Shtukenberg, E. Gunn, M. Gazzano, J. Freudenthal, E. Camp, R. Sours, E. Rosseeva and B. Kahr, *ChemPhysChem*, 2011, **12**, 1558–1571.
17 A. G. Shtukenberg, Y. O. Punin, A. Gujral and B. Kahr, *Angew. Chem., Int. Ed.*, 2014, **53**, 672–699.
18 A. G. Shtukenberg, J. Freudenthal and B. Kahr, *J. Am. Chem. Soc.*, 2010, **132**, 9341–9349.
19 A. G. Shtukenberg, A. Gujral, E. Rosseeva, X. Cui and B. Kahr, *CrystEngComm*, 2015, **17**, 8817–8824.
20 M. More, G. Odou and J. Lefebvre, *Acta Crystallogr., Sect. B: Struct. Sci.*, 1987, **43**, 398–405.
21 I. Olson, G. Hakobyan, A. G. Shtukenberg, A. Rohl, P. Raeteri, M. D. Ward and B. Kahr, *J. Phys. Chem. Lett.*, 2016, **7**, 3112–3117.
22 J. Wang, R. M. Wolf, J. W. Caldwell, P. A. Kollman and D. A. Case, *J. Comput. Chem.*, 2004, **25**, 1157–1174.
23 A. Nemkevich, H.-B. Bürgi, M. A. Spackman and B. Corry, *Phys. Chem. Chem. Phys.*, 2010, **12**, 14916–14929.
24 S. Plimpton, *J. Comput. Phys.*, 1995, **117**, 1–19.
25 E. Vanquelef, S. Simon, G. Marquant, E. Garcia, G. Klimerak, J. C. Delepine, P. Cieplak and F.-Y. Dupradeau, *Nucleic Acids Res.*, 2011, **39**, W511–W517.
26 F. Wang, J. P. Becker, P. Cieplak and F. Y. Dupradeau, *R.E.D. Python: Object oriented programming for Amber force fields*, Université de Picardie–Jules Verne, Sanford Burnham Prebys Medical Discovery Institute, 2013.
27 F. Y. Dupradeau, A. Pigache, T. Zaffran, C. Savineau, R. Lelong, N. Grivel, D. Lelong, W. Rosanski and P. Cieplak, *Phys. Chem. Chem. Phys.*, 2010, **12**, 7821–7839.
28 C. I. Bayly, P. Cieplak, W. Cornell and P. A. A. Kollman, *J. Phys. Chem.*, 1993, **97**, 10269–10280.
29 J. D. Gale and A. L. Rohl, *Mol. Simul.*, 2003, **29**, 291–341.
30 J. D. Gale, *Z. Kristallogr. - Cryst. Mater.*, 2005, **220**, 552–554.
31 E. Efrati, *Isr. J. Chem.*, 2020, **60**, 1185–1189.